Z. Phys. A - Atoms and Nuclei 302, 133–142 (1981)

Zeitschrift für Physik A Atoms and Nuclei

Nuclear Interactions of 4.5 GeV/c Protons in Emulsion and the Cascade-Evaporation Model

Alma-Ata - Bucharest - Dubna - Dushanbe - Kishinev - Košice - Leningrad - Moscow - Tashkent - Ulaan-Bator Collaboration

V.I. Bubnov, A.Sh. Gaitinov, L.E. Eremenko, B. Kusambaev, and I.Ya. Chasnikov
Institute of High Energy Physics, Alma-Ata, USSR

M. Marku, A. Marin, and M. Khaiduk
Institute for Atomic Physics, Bucharest, Romania

B.P. Bannik, V.V. Ivanov, B.F. Kostenko, V.A. Leskin, K.D. Tolstov, M. Shumbera, and S. Vokal
Joint Institute for Nuclear Researches, Dubna, USSR

L. Akhmadalieva
Tajik State University, Dushanbe, USSR

Yu.P. Keloglu
Moldavian State University, Kishinev, USSR

M. Karabova, Ya. Karaba, V. Novicki, E. Sileš, and M. Totova
Safarik University, Košiće, Czechoslovakia

V.G. Bogdanov, N.A. Perfilov, V.A. Plyushev, and Z.I. Solovieva
V.G. Khlopin Radium Institute, Leningrad, USSR

V.A. Antonchik, V.A. Bakaev, S.D. Bogdanov, and V.I. Ostroumov
Leningrad Polytechnik Institute, Leningrad, USSR

M.I. Adamovich, V.G. Larionova, and S.P. Kharlamov
P.N. Lebedev Physical Institute, Moscow, USSR

E.S. Basova, R.A. Bondarenko, U.G. Gulyamov, R.M. Ibatov, M.M. Muminov, B.G. Rakhimbaev, and G.M. Chernov
Institute of Nuclear Physics, Ulugbek, Tashkent, USSR

S.A. Azimov and K.G. Gulamov
S.V. Starodubtsev Physical Technical Institute, Tashkent, USSR

N. Dalkhazhav*, R. Togoo, and B. Chadraa
Institute of Physics, Ulaan-Bator, Mongolia

Received February 26, 1981

New experimental data on proton-nucleus interactions in emulsion at primary momentum 4.5 GeV/c are presented and discussed. The data are systematically compared with predictions of the cascade-evaporation model. The directions of development of the cascade-evaporation model in a region of incident momenta are considered, and some suggestions are made for giving it more precision.

* Deceased

0340-2193/81/0302/0133/$02.00

1. Introduction

It is now commonly believed that the study of multiparticle production on nuclei will enable us to clarify the space-time structure of production process at very short ($\sim 10^{-13}$ cm) internucleonic distances in nuclei and also to investigate local properties of strong interactions. Most of the existing experimental data on hadron-nucleus (hA) interactions have been acquired at energies that are high enough ($E_0 > 10$ GeV) for effects connected with formation lengths of hadrons to come into play and where a trivial branchy intranuclear cascade no longer describes characteristics of hA collisions.

In the region of relatively low energies, the experimental and theoretical situation is characterized by a great deal of uncertainty. There are no theoretical approaches, except a cascade-evaporation model (CEM) highly developed in the quantitative respect, which may pretend to describe a more or less wide variety of hA interaction characteristics. On the other hand, it is obviously important to know to which energies normal cascade notions about the mechanisms of nuclear production work well.

The aim of the present is twofold: first, to obtain new experimental information about different characteristics of proton-nucleus (pA) interactions in emulsion at primary momentum $p_0 = 4.5$ GeV/c* and, second, to perform detailed quantitative comparison of these data with predictions of the cascade-evaporation model.

2. Experimental Procedures

In the present experiment, stacks of GOSNIIHIMFOTOPROEKT BR-2 emulsions of dimension 10×20 cm^2 and 600 μ thick were exposed to a 4.5 GeV/c proton beam at the Synchrophasotron of JINR, Dubna. The intensity of the exposure was 2×10^4 protons/cm^2.

Along the track double scanning was carried out, fast in the forward and slow in the backward direction. The one-prong events, with an emission angle of secondary particle $\theta < 5°$ and no visible tracks from excitation or disintegration of target nucleus, were excluded as they were considered to be due to the elastic scattering. The mean free path for inelastic pA interactions in emulsion was found to be $\lambda = (30.2 \pm 0.7)$ cm. For a further analysis 2576 inelastic interactions of protons in emulsion were used.

The charged secondary particles were divided according to the standard photoemulsion criteria into the following groups:

1. s-particles: relativistic particles of relative ionization $g/G < 1.4$ (corresponding proton energy $T_p > 400$ MeV), where G is ionization measured at the primary proton track;

2. g-particles: with ionization $g/G > 1.4$ and range in emulsion $R > 3000$ μ (corresponding energy of protons $400 > T_p > 26$ MeV);

3. b-particles: with range $R \leqq 3000$ μ.

For *g* and *b*-particles in the whole a name heavily ionizing or *h*-particles is used and $n_h = n_g + n_b$ holds for their multiplicity.

Part of our statistics determined the characteristics of heavily ionizing tracks. Energies of *g*-tracks were found by range and/or relative ionization measurements (assuming that they are protons). Determination of *b*-particle energies was carried out by measuring a range of a given track and using known dependencies $E = f(R_{p,\alpha})$. Charge identification of *b*-tracks was performed for the tracks with a dip angle $\alpha \leqq 30°$ according to dependence of the number of gaps on a track on the residual range. Calibration curves were obtained on π^+-mesons, protons, α-particles and ^{8}Li nuclei tracks. In a process of identification a dip angle of the track and its place in stack were taken into account [5].

3. Cascade-Evaporation Model

The cascade-evaporation model of hA interactions has been quantitatively developed in many papers of which a detailed review and further generalization may be found in a monograph [6]. Calculations used in the present work have been performed in the framework of variant of CEM, which takes into account the decrease of nuclear density in the process of the development of cascading stage (the so-called trailing-effect [7]). The contribution of non-stationary process of decay of excited residual nucleus, which precedes the evaporation stage of formation of secondary particles, was also taken into account. This part of the calculations was performed in accordance with other papers [8–10].

For the calculation of input characteristics of intranuclear pion-nucleon (πN) and nucleon-nucleon (NN) interactions the method described in refs. [6, 11] was applied. This method is supposed to approximate separately angular and momentum spectra of secondaries produced in hN collisions and the distribution of their transverse momenta reasonably well.

Calculations were performed by the Monte Carlo simulation of random stars (a total of 4879 inelastic events were generated) with the composition of nuclear emulsion used taken into account. In the next step these random stars were proceeded in the exact

* Present work is continuation of experiments of our collaboration investigating nucleus-nucleus interactions in emulsion at 4.5 GeV/c per nucleon [1–4]

accordance with criteria used for the analysis of experimental material.

4. Multiplicities of Various Types of Charged Secondaries

Our main experimental results concerning the multiplicity of various types of secondaries are presented in Table 1 and Figs. 1–4. Table 1 contains the experimental data on the average values of the multiplicity for different groups of pA interactions in emulsion* at 4.5 GeV/c in comparison with the predictions of CEM. In Fig. 1 we have plotted, in matrix form, the frequency of analysed stars depending on the number of s-, g- and b-tracks, which fully characterizes the corresponding multiplicity distributions. Finally, in Figs. 2–4, multiplicity distributions of s-, g- and b-particles are exhibited in comparison with the results of CEM calculations.

The analysis of these data allows the following conclusions to be made:

1. CEM quite satisfactorily reproduces the average multiplicities of s- and g-particles in all considered groups of pA interactions in emulsion. With regard to b-particles, the model systematically underestimates their average multiplicity and discrepancy

* It should be noted that pA interactions with $n_h \leqq 6$ consist of collisions on light emulsion nuclei (p-HCNO) and of peripheral interactions on heavy nuclei (p-AgBr). Events having $n_h > 15$ can be conditionally considered as central collisions of incident protons with AgBr nuclei

Table 1. Average multiplicities of charged secondary particles in different groups of pA interactions in emulsion at 4.5 GeV/c in comparison with predictions of the CEM

Group of events	$\langle n_s \rangle$	$\langle n_g \rangle$	$\langle n_b \rangle$	Number of events	
All pA collisions	1.63 ± 0.02	2.81 ± 0.06	3.77 ± 0.08	2576	exp
	1.75	2.71	3.29	4879	CEM
Events with $n_h \leqq 6$	1.68 ± 0.03	1.21 ± 0.03	1.39 ± 0.04	1602	exp
	1.80	1.14	1.00	3014	CEM
Events with $6 < n_h \leqq 15$	1.66 ± 0.04	4.40 ± 0.08	5.96 ± 0.09	689	exp
	1.78	4.41	5.72	1440	CEM
Events with $n_h > 15$	1.29 ± 0.06	7.96 ± 0.15	11.8 ± 0.2	285	exp
	1.31	8.02	11.29	425	CEM

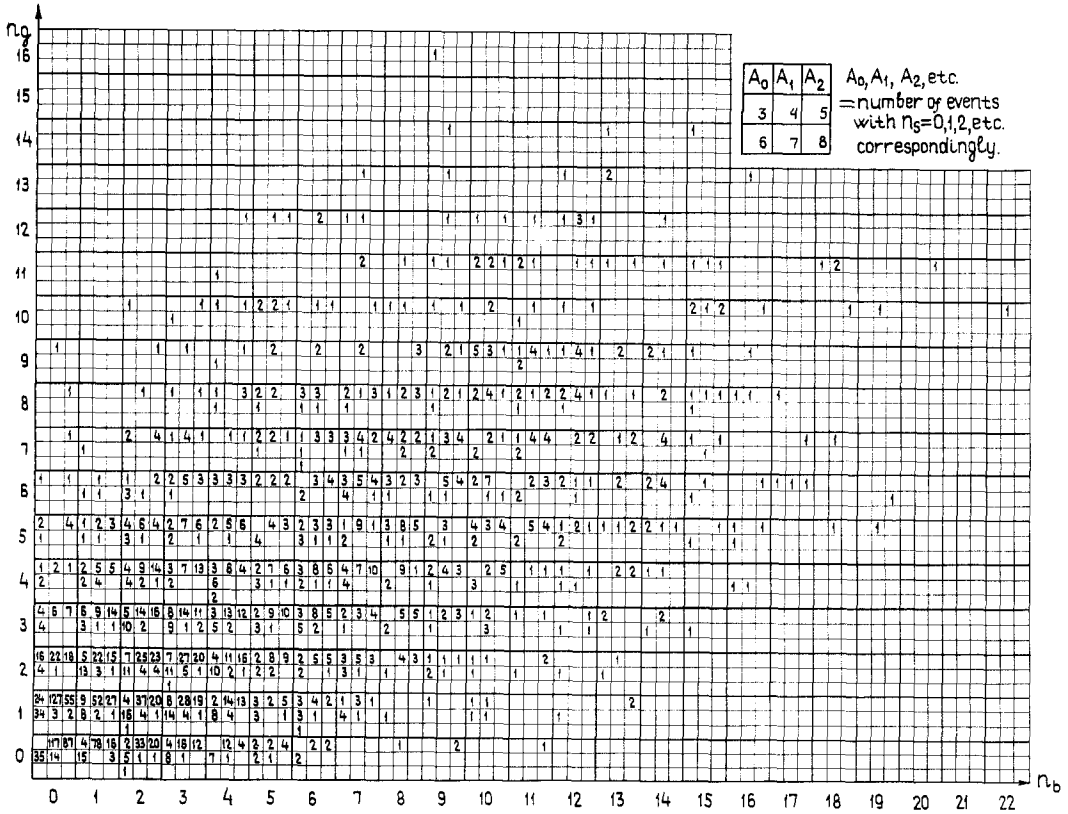

Fig. 1. The frequency of pA interactions in emulsion at 4.5 GeV/c in dependence of the multiplicity of s-, g- and b-particles

becomes essential for $n_h \leqq 6$ group of events. One can assume that this circumstance is related to the fact that the latter group is enriched by collisions with light (HCNO) emulsion nuclei, which constitute approximately 50% of all interactions in this group of events.

2. The model describes n_s-distributions satisfactorily and multiplicity distributions of g-particles reasonably well (Figs. 2, 3).

3. The experimental data on multiplicity distributions of b-particles disagree with results of calcu-

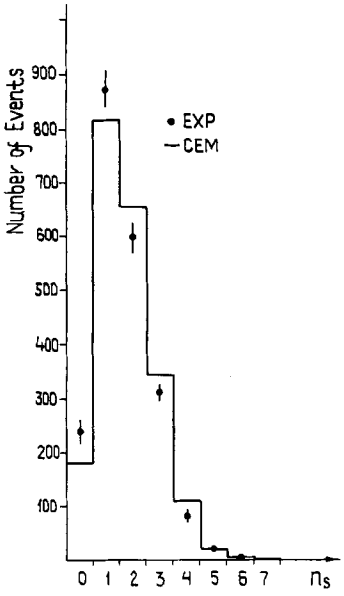

Fig. 2. Multiplicity distribution of relativistic particles in pA interactions at 4.5 GeV/c. The solid histogram is the CEM prediction

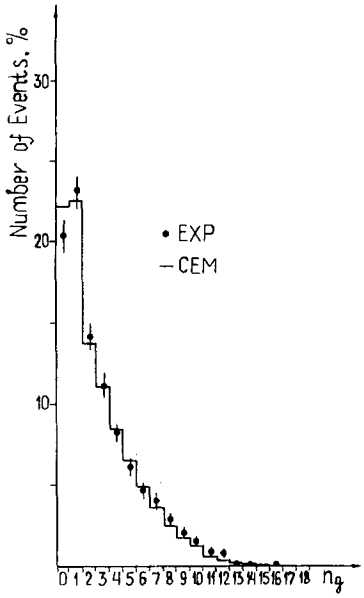

Fig. 3. n_g-distribution in pA interactions in comparison with the CEM predictions

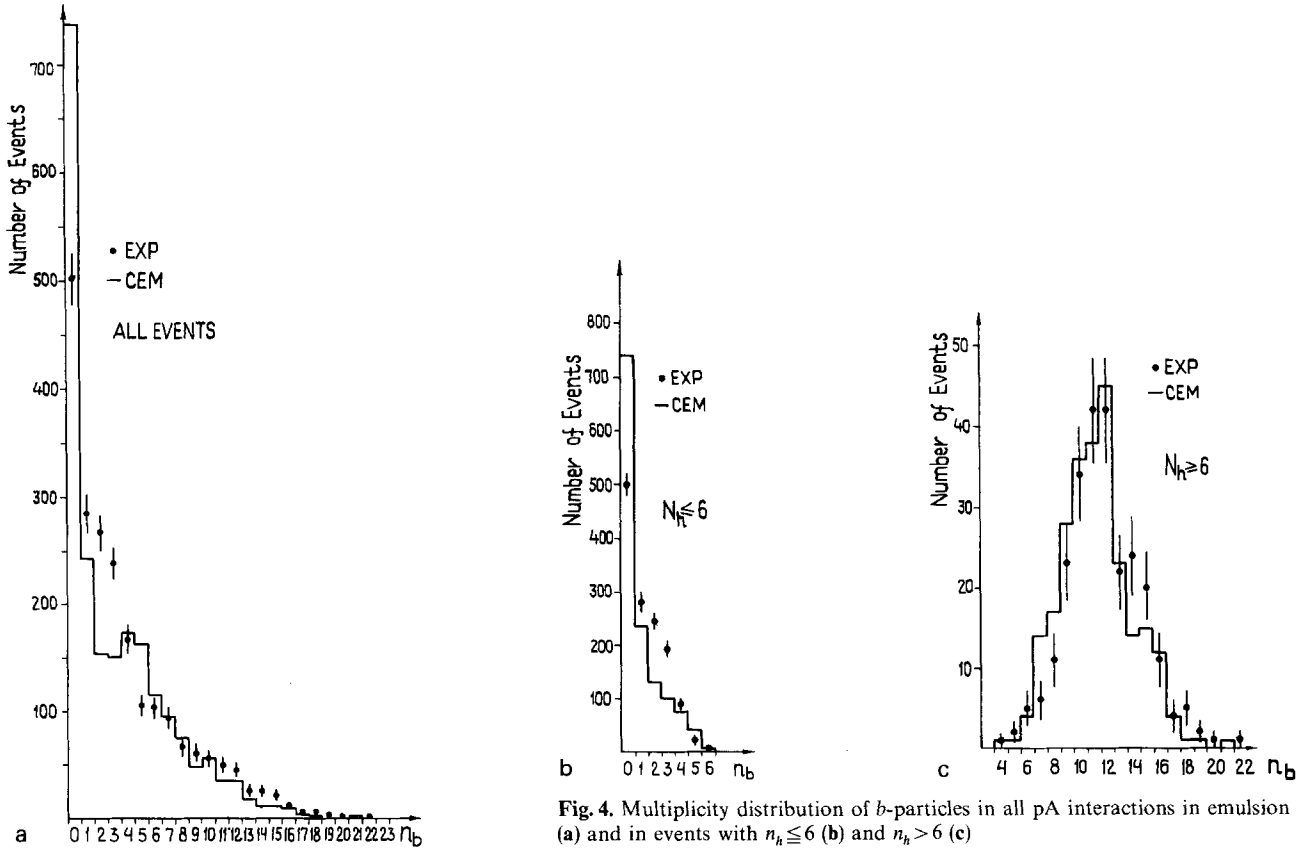

Fig. 4. Multiplicity distribution of b-particles in all pA interactions in emulsion (**a**) and in events with $n_h \leqq 6$ (**b**) and $n_h > 6$ (**c**)

lations performed in the considered framework of a variant of CEM (Figs. 4a, b, c). Of course, it should be noted that for central collisions of protons with heavy emulsion nuclei (AgBr), the predictions of CEM may turn out to be close to reality. This is true when the number of intranuclear collisions is large enough and the process of formation of slow secondaries, products of target fragmentation, is 'thermolyzed' and acquires a pronounced statistical character.

The study of correlation dependences between multiplicities of different types of secondary particles may be of considerable importance for understanding mechanisms of hA interactions at the energies considered. Some typical examples of such dependences for pA collisions at 4.5 GeV/c are shown in Figs. 5–7, analysis of which allows us to draw three conclusions:

a) In the region of not very high multiplicities ($n_i \lesssim 10$) correlation dependences can be satisfactorily approximated by linear functions

$$\langle n_i(n_j)\rangle = a_{ij} + b_{ij} n_j, \tag{1}$$

parameters of which were presented by us in an earlier publication [12].

b) In contrast to the region of high primary momenta ($p_0 > 10$ GeV/c), the multiplicity of *s*-particles in pA collsions at 4.5 GeV/c decreases with the increase of n_g and n_b. This fact can be considered as an indication of the absence of noticeable meson production in secondary intranuclear processes and of absorption of relativistic particles with decreasing impact parameter of hA collisions and/or with increasing number of intranuclear collisions. It should be noted that at the same time the multiplicities of particles characterizing the degree of excitation of

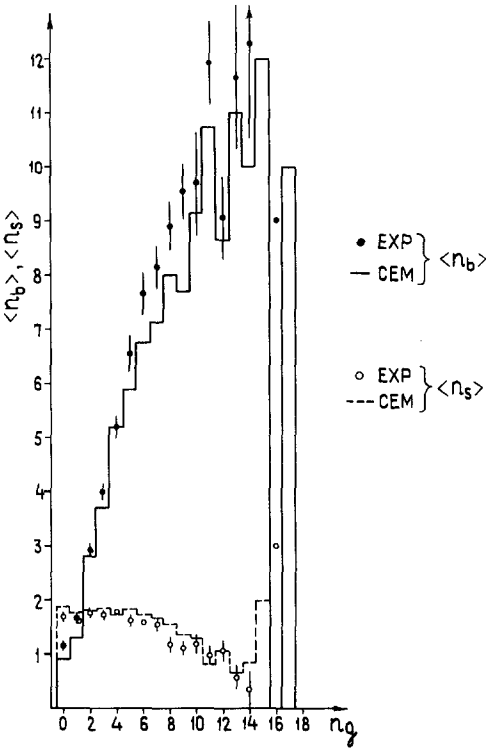

Fig. 6. Multiplicity correlations $\langle n_b(n_g)\rangle$ and $\langle n_s(n_g)\rangle$

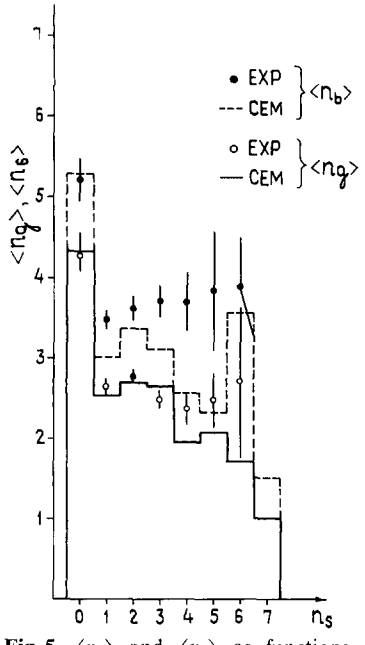

Fig. 5. $\langle n_g\rangle$ and $\langle n_b\rangle$ as functions of n_s in pA collisions at 4.5 GeV/c

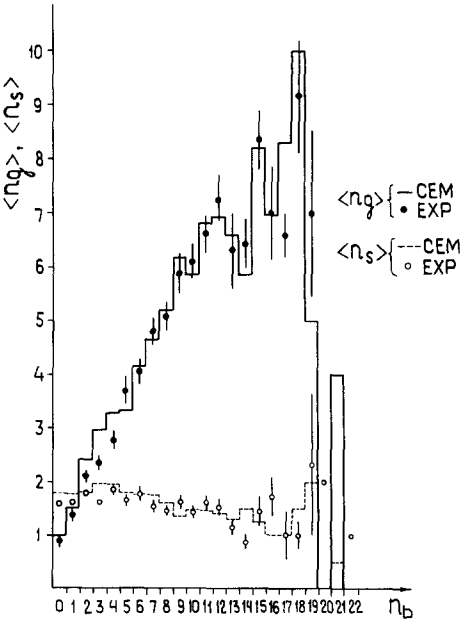

Fig. 7. Multiplicity correlations $\langle n_g(n_b)\rangle$ and $\langle n_s(n_b)\rangle$

target nucleus weakly depend on the number of relativistic particles, except of a point $n_s=0$, where one has for instance $\langle n_h\rangle=9.5\pm0.5$.

c) The observed behaviour of multiplicity correlations can be easily understood if one takes into account that at the energies considered characteristics of hA collisions are strongly influenced by the action of two competing factors. The first is conditioned by the multiplication of relativistic particles due to cascading. The second is related to the rapid dissipation of not very high primary energy resulting from intranuclear collisions and by absorption of relativistic particles within the nucleus. In fact, effective production of relativistic particles in cascade rescatterings at the energy used by us is damped by energetic reasons, owing to the action of energy-momentum conservation. As both factors are taken into account in CEM, in general it satisfactorily describes qualitative features of the experimental data on multiplicity correlations. It should be noted, of course, that CEM systematically overestimates correlations of the type $\langle n_b(n_j)\rangle$ that is obviously related to the above-mentioned discrepancy in describing the average multiplicity of *b*-particles.

5. Angular Distributions of Relativistic Particles

The main experimental data characterizing angular distribution of relativistic particles in different groups of pA interactions considered in pseudorapidity variable $\eta=\ln\mathrm{ctg}(\theta/2)$ (θ being the polar angle in the laboratory frame) are presented in Table 2 and Figs. 8a, b, c. The corresponding predictions of CEM are also given; note that for the convenience of the following discussion we also show the separate contributions of $\pi^{\pm}$-mesons and protons into angular distributions of relativistic particles in the model.

One can conclude from the data presented that:

i) As is the case of very high energy hA interactions (see, e.g. the review [13]), in pA collisions at 4.5 GeV/c the average values of pseudorapidities for relativistic particles decrease with increasing number of heavily ionizing fragments of the target characterizing the degree of disintegration of the nucleus and/or the number of intranuclear collisions. At the same time dispersions of angular distributions weakly depend on n_h (decrease for relativistic protons). CEM reproduces qualitative features of angular spectra of relativistic particles reasonably well. It is important to note that, as the results of calculations show, in the framework of CEM the features of η-distributions discussed are inherent to both $\pi^{\pm}$-mesons and relativistic protons separately.

ii) At small values of η, i.e. in the target fragmentation region, the model describes the angular distributions well and the main contribution comes from $\pi^{\pm}$-mesons (Fig. 8a). Concerning the projectile fragmentation region, where relativistic protons give the main contribution into angular spectra of relativistic particles, the CEM does not describe the data: predictions of CEM are systematically lower than the experimental points. In general the CEM does not quantitatively reproduce η-distributions of relativistic particles produced in 4.5 GeV/c pA interactions.

In the framework of the model itself the discrepancy observed can be attributed to the action of two basic factors: (1) it may be related with bad reproduction of the input data on elementary intranuclear πN and NN interactions used in CEM, i.e. with the bad account of elementary act characteristics in CEM, and (2) it is possible that in multiparticle production processes effects related to the increase of hadron's formation lengths start to manifest themselves at 4.5 GeV/c. Because attention was not paid to these effects in CEM, the model can overestimate the degree of development of intranuclear collisions of

Table 2. Average values of pseudorapidities and dispersions (σ) of pseudorapidity distrubutions of relativistic particles in different n_h-groups of pA collisions in comparison with the CEM predictions

Group of events		$n_h\leqq6$	$6<n_h\leqq15$	$n_h>15$	All pA collisions
Experimental data	$\langle\eta_s\rangle$	1.87 ± 0.02	1.22 ± 0.03	0.81 ± 0.05	1.61 ± 0.02
	σ_s	1.36 ± 0.05	0.98 ± 0.06	0.85 ± 0.12	1.35 ± 0.04
Predictions of CEM for different types of relativistic particles	$\langle\eta_s\rangle$	1.74	1.22	0.88	1.52
	σ_s	0.93	1.03	1.02	1.05
	$\langle\eta_s\rangle_{\pi^{\pm}}$	1.32	0.85	0.67	1.11
	$\sigma_{s\pi^{\pm}}$	1.12	1.49	0.98	1.02
	$\langle\eta_s\rangle_p$	2.18	1.81	1.61	2.09
	σ_{sp}	1.05	0.81	0.58	0.83

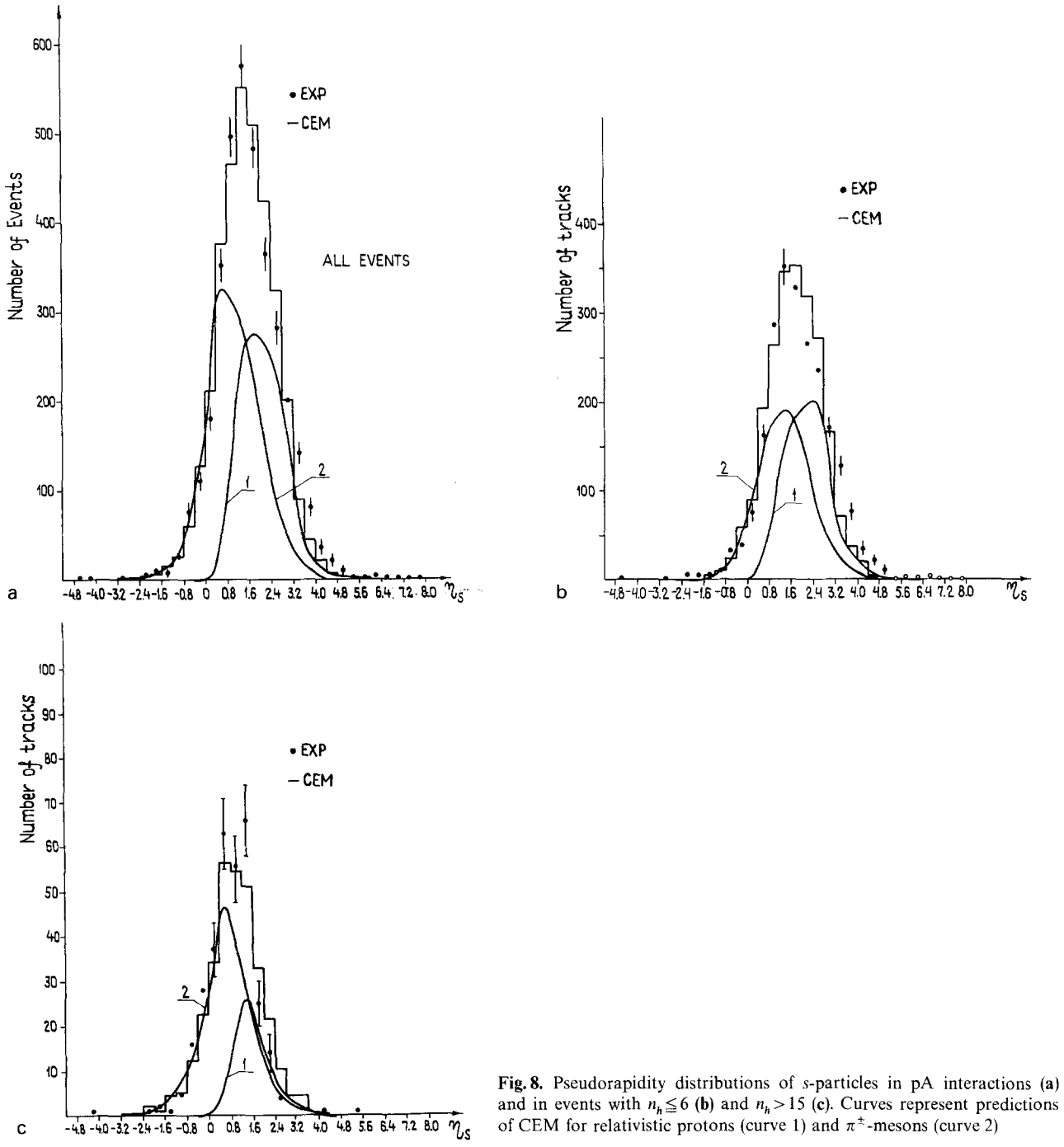

Fig. 8. Pseudorapidity distributions of s-particles in pA interactions (**a**) and in events with $n_h \leqq 6$ (**b**) and $n_h > 15$ (**c**). Curves represent predictions of CEM for relativistic protons (curve 1) and $\pi^{\pm}$-mesons (curve 2)

produced particles, i.e. the degree of cascade multiplication of particles.

The proper choice between these two possibilities seems to be a rather difficult task because of scarcity of precise data on πN and NN interactions below 4.5 GeV/c. Nevertheless, we have tried to get information, though indirect, about the influence of these factors by looking at the experimental data for two groups of pA collisions having $n_h \leqq 6$ and $n_h > 15$ (Figs. 8b, c respectively). It is obvious that the first group of events is enriched by interactions that are close to hN collisions, whereas the second group practically does not contain them.

One can see from Fig. 8b that for the $n_h \leqq 6$ group the observed disagreement between the data and the CEM predictions in the projectile fragmentation region becomes stronger, which is to be expected if the effect arises due to the bad quality of elementary hN collisions. On the other hand, for the $n_h > 15$ group (Fig. 8c) the situation in the projectile fragmentation

region changes qualitatively - the CEM predictions now become systematically higher than the experimental data; it is interesting that at the same time the contribution of produced $\pi^{\pm}$-meansons in that kinematic region turns out to be comparable with the contribution of relativistic protons.

Such behaviour of angular spectra allows us to conclude that an insufficiently correct account of elementary act characteristics in the framework of CEM plays a considerable role in the observed disagreement between the data and the model predictions. However, bearing in mind the results obtained for the $n_h > 15$ group, the second factor, which is related with the possible overestimation of the cascade multiplication of produced particles, also contributes to the discrepancy observed. Due to the importance of the problem for the theory of multiparticle production on nuclei, this question needs further investigations.

6. Characteristics of Heavily Ionizing Particles

In Table 3 data are presented on the average characteristics of angular distributions for heavily ionizing particles in considered pA interactions. Note that values of the ratio of multiplicities of particles emitted forwards and backwards in the laboratory frame (F/B) are listed not only for all b-particles, but also for identified protons and α-particles.

In pA interactions at 4.5 GeV/c the angular distributions of g and b-particles (not illustrated) do not have any peculiarities and turn out to be anisotropic in the laboratory frame. The anisotropy of angular distributions for all types of heavily ionizing particles weakly decreases with an increase of their multiplicities, whereas the dispersion of g-particles angular distribution weakly increases indicating the importance of secondary rescatterings of g-particles within the target nucleus. One can see from Table 3 that these features of angular distributions are reproduced quite well by the CEM.

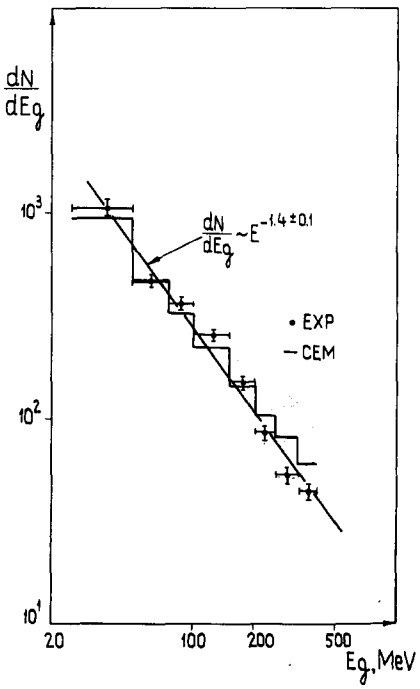

Fig. 9. The energy spectrum of g-particles. The histogram represents predictions of CEM

In Fig. 9 we show the energy spectrum of g-particles that can be approximated by the simple dependence

$$\frac{dN}{dE_g} \sim E_g^{-\alpha}, \tag{2}$$

with the value of parameter $\alpha = 1.4 \pm 0.1$. The value of parameter α appears to be stable with respect to the change of primary energy. It has been shown [6] that for emulsion nuclei in the range 3-26 GeV one has $\alpha = 1.55 \pm 0.20$. As one can see from Fig. 9, the distribution calculated following CEM describes the data well enough, except for a region $E_g > 200$ MeV,

Table 3. Characteristics of angular distributions of heavily ionizing particles in different groups of pA interactions in comparison with predictions of the CEM

Group of events	$n_h \leq 6$	$6 < n_h \leq 15$	$n_h > 15$	$n_h > 6$	All pA collisions	
$\langle \cos \theta_g \rangle$	0.36 ± 0.01	0.30 ± 0.01	0.28 ± 0.01	0.30 ± 0.01	0.32 ± 0.01	exp
	0.39	0.31	0.29	0.30	0.32	CEM
Asymmetry (F/B) for protons from b-particles	1.2 ± 0.2	1.1 ± 0.1	1.1 ± 0.1	1.00 ± 0.1	1.1 ± 0.1	exp
	1.3	1.1	1.2	1.2	1.2	CEM
(F/B) for α-particles from b-particles	2.0 ± 0.4	1.5 ± 0.3	1.2 ± 0.2	1.3 ± 0.2	1.5 ± 0.1	exp
	1.3	1.2	1.2	1.2	1.2	CEM
(F/B) for all b-particles	1.3 ± 0.1	1.3 ± 0.1	1.2 ± 0.1	1.3 ± 0.1	1.3 ± 0.1	exp
	1.4	1.2	1.2	1.2	1.2	CEM

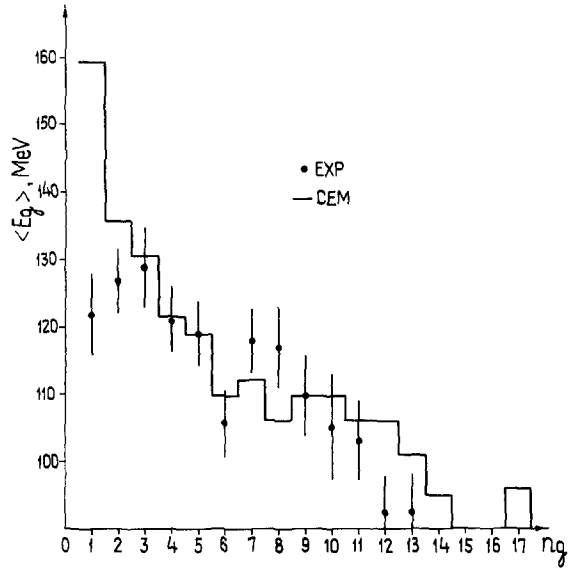

Fig. 10. Average energy of g-particles as a function of the multiplicity n_g

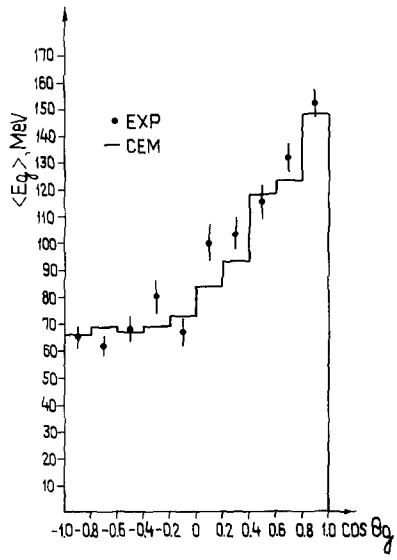

Fig. 11. The angular dependence of the average energy of g-protons in pA collisions at 4.5 GeV/c

Table 4. Average energies of heavily ionizing particles in different n_h groups of pA collisions at 4.5 GeV/c in comparison with CEM predictions

Group of events	$n_h \leqq 6$	$6 < n_h \leqq 15$	$n_h > 15$	All pA collisions	
$\langle E_g \rangle$ in MeV	122 ±5	110 ±4	103 ±5	112 ±3	exp
	146	117	105	121	CEM
$\langle E_b \rangle_p$ in MeV	8.8±0.4	10.4±0.3	9.7±0.4	9.7±0.2	exp
	10.7	11.6	12.4	11.7	CEM
$\langle E_b \rangle_\alpha$ in MeV	19.4±1.7	23.5±1.5	23.5±1.3	22.6±0.8	exp
	11.9	15.1	16.2	14.6	CEM
Comparative yield of α-particles and protons among b-particles $(\alpha/p)_b$	0.44±0.05	0.40±0.04	0.55±0.05	0.46±0.03	exp
	0.16	0.10	0.12	0.11	CEM

where the model overestimates the multiplicity of g-particles. It is interesting that, as seen from the data of Table 4, the average energy of g-particles weakly decreases with the increase of the degree of disintegration of the target nucleus, corresponding well with the observed changes in their angular characteristics (see Table 3).

It is interesting that the average energies of g-particles depend on their multiplicity (Fig. 10). This fact may be related with both the conservation of primary energy (not very high in our case) and dissipation of energy of g-particles in the course of their rescatterings within the target nucleus. From Fig. 10 one can conclude that CEM successfully describes this feature of the energy spectrum of g-particles, with the exception of events with $n_g = 1$, a considerable number of which are interactions very close to the input elementary collisions.

In Fig. 11 we have illustrated the dependence of the average energy of g-protons on the angle of their emission. It is seen that while in the forward hemisphere in the laboratory frame the average energy essentially depends on $\cos\theta_g$ (increases with increasing $\cos\theta_g$), in the backward hemisphere $\langle E_g \rangle$ is practically independent of $\cos\theta_g$. CEM describes this property of g-protons reasonably well. One may also note that the momentum spectrum of g-protons having $\cos\theta_g < -0.2$ and $E_g < 200$ MeV can be well parametrized by the dependence of the type $C \times \exp(-Bp^2)$ with the value of parameter $B = (12.6 \pm 1.8)$ $(\text{MeV/c})^{-2}$, that agrees well with the result following for such particles from the cascade-evaporation model $B = (12.5 \pm 1.5)$ $(\text{MeV/c})^{-2}$.

Finally, for b-particles one can note some increase of $\langle E_p \rangle$ and $\langle E_\alpha \rangle$ for events with $n_h > 7$ that is probably related with the influence of Coulomb barrier. It is also seen from Table 4 that CEM satisfactorily describes these data with the exception of $\langle E_g \rangle$ for low-multiplicity events having $n_h \leqq 6$. It is important, however, that the model does not reproduce the

comparative yields of protons and α-particles among b-particles (see the last line in Table 4). In the CEM this is related to both the inadequate account of the nuclear structure effects (for instance, the existence of intranuclear clusters is completely ignored) and the practical neglect of final state interactions (coalescence) which led to the increase of the yield of complex fragments.

7. Conclusions

In this paper experimental data is given on various general characteristics of pA interactions in emulsion at 4.5 GeV/c. The data have been systematically compared with predictions of the CEM.

Cascade phenomena in pA interactions at the energy considered play the decisive role and the CEM correctly reproduces the qualitative time-flow of the interaction process. With this we have found a number of quantitative disagreements between the data and model predictions. In our opinion, the most serious among them are discrepancies for characteristics, of both heavily ionizing and relativistic particles, in interactions with light emulsion nuclei. These discrepancies probably originate from the crudeness of the evaporation approach used in the model and the inaccurate account of the characteristics of input intranuclear collisions.

We feel that effects related with the formation lengths of particles produced probably also contribute. The importance of the problem is related to the fact that it is so far unknown at exactly what energy for the fixed target nucleus the growth of formation lengths for produced particles would destroy the applicability of the CEM. In order to clarify this question quantitatively, it is neccessary to compare more detailed experimental data (especially for newly produced particles and for fixed target nuclei) with predictions of CEM under more exact reproduction of characteristics of elementary intranuclear collisions. In order to describe the target fragmentation in the model, it is also necessary to consider more carefully effects connected with the details of nuclear structure together with final state interactions. These modifications can be introduced into the CEM without change of its basic postulates.

We would like to express our gratitude to the synchrophasotron group of JINR for the exposure and to S.I. Lubomilov and members of his team for preparing and processing the plates. The work carried out by the technical staff of our laboratories is gratefully acknowledged.

References

1. Bogachev, N.I., et al.: JINR report P1-6877, Dubna (1972)
2. Galstyan, J.A., et al.: Nucl. Phys. A **208**, 628 (1973)
3. Tolstov, K.D., et al.: JINR report P1-8313, Dubna (1974)
4. Shabratova, G.S., et al.: Acta Phys. Slov. **28**, 132 (1978)
5. Serebryannikov, Yu.I.: Scientific bulletin of phys. and math. sciences N°12, M.I., Kalinin Leningrad Polytechnic Institute, Leningrad (1957)
6. Barashenkov, V.S., Toneev, V.D.: "Interactions of high energy particles and atomic nuclei with nuclei", Atomizdat, Moscow (1972)
7. Barashenkov, V.S., et al.: Yad. Fiz. **13**, 743 (1971)
8. Gudima, K.K., et al.: JINR report P4-7821, Dubna (1974)
9. Mashnik, S.G., Toneev, V.D.: JINR report P4-8417, Dubna (1974)
10. Barashenkov, V.S., et al.: Acta Phys. Pol. B **10**, 607 (1979)
11. Artykov, I.Z., et al.: Acta Phys. Pol. B **11**, 39 (1980)
12. Bannik, B.P., et al.: JINR report P1-13055, Dubna (1980)
13. Gulamov, K.G., et al.: Fiz. Elem. Chastits At. Yadra **9**, 554 (1978)

K.G. Gulamov
Laboratory of High Energy Physics
Physical Technical Institute
Timiryazeva 2
Tashkent 700084
USSR